Phage-antibiotic combination is a superior treatment against *Acinetobacter baumannii* in a preclinical study

Fernando L. Gordillo Altamirano,[a,b,f] Xenia Kostoulias,[b,c] Dinesh Subedi,[a,b] Denis Korneev,[d,e] Anton Y. Peleg,[b,c,f]* and Jeremy J. Barr[a,b]*

[a]School of Biological Sciences, Monash University, Clayton, Victoria, Australia
[b]Centre to Impact AMR, Monash University, Clayton, Victoria, Australia
[c]Infection Program, Department of Microbiology Monash University, Monash Biomedicine Discovery Institute, Clayton, Victoria, Australia
[d]Department of Biochemistry and Molecular Biology, Biomedicine Discovery Institute, Monash University, Clayton, Victoria, Australia
[e]Faculty of Science, School of BioSciences, University of Melbourne, Melbourne, Victoria, Australia
[f]Department of Infectious Diseases, The Alfred Hospital and Central Clinical School, Monash University, Melbourne, Victoria, Australia

eBioMedicine 2022;80: 104045
Published online xxx
https://doi.org/10.1016/j.ebiom.2022.104045

Summary

Background Clinical phage therapy is often delivered alongside antibiotics. However, the phenomenon of phage-antibiotic synergy has been mostly studied *in vitro*. Here, we assessed the *in vivo* bactericidal effect of a phage-antibiotic combination on *Acinetobacter baumannii* AB900 using phage øFG02, which binds to capsular polysaccharides and leads to antimicrobial resensitisation *in vitro*.

Methods We performed a two-stage preclinical study using a murine model of severe *A. baumannii* AB900 bacteraemia. In the first stage, with an endpoint of 11 h, mice (n = 4 per group) were treated with either PBS, ceftazidime, phage øFG02, or the combination of phage and ceftazidime. The second stage involved only the latter two groups (n = 5 per group), with a prolonged endpoint of 16 h. The primary outcome was the average bacterial burden from four body sites (blood, liver, kidney, and spleen). Bacterial colonies from phage-treated mice were retrieved and screened for phage-resistance.

Findings In the first stage, the bacterial burden (CFU/g of tissue) of the combination group (median: 4.55×10^5; interquartile range [IQR]: 2.79×10^5–2.81×10^6) was significantly lower than the PBS (median: 2.42×10^9; IQR: 1.97×10^9–3.48×10^9) and ceftazidime groups (median: 3.86×10^8; IQR: 2.15×10^8–6.35×10^8), but not the phage-only group (median: 1.28×10^7; IQR: 4.71×10^6–7.13×10^7). In the second stage, the combination treatment (median: 1.72×10^6; IQR: 5.11×10^5–4.00×10^6) outperformed the phage-only treatment (median: 7.46×10^7; IQR: 1.43×10^7–1.57×10^8). Phage-resistance emerged in 96% of animals receiving phages, and all the tested isolates (n = 11) had loss-of-function mutations in genes involved in capsule biosynthesis and increased sensitivity to ceftazidime.

Interpretation øFG02 reliably drives the *in vivo* evolution of *A. baumannii* AB900 towards a capsule-deficient, phage-resistant phenotype that is resensitised to ceftazidime. This mechanism highlights the clinical potential of using phage therapy to target *A. baumannii* and restore antibiotic activity.

Funding National Health and Medical Research Council (Australia).

Keywords: Acinetobacter baumannii; Phage therapy; Antimicrobial resistance; Phage-resistance; Ceftazidime; Preclinical study; Synergism

*Corresponding authors at: Centre to Impact AMR, Monash University, Clayton, Victoria, Australia.
E-mail addresses: anton.peleg@monash.edu (A.Y. Peleg), jeremy.barr@monash.edu (J.J. Barr).

Introduction

Antimicrobial resistance (AMR) is considered one of the biggest threats to global health. While the COVID-19 pandemic has rekindled the world's interest in the

Research in context

Evidence before this study

Acinetobacter baumannii has been named a critical priority for the research and development of new therapeutic strategies. A search in PubMed in September 2021, with no restrictions by date or language, using the search terms "*Acinetobacter baumannii*" AND "phage therapy", and excluding review articles, obtained 66 results. A manual assessment of these articles looked for either clinical case reports, preclinical models, and/or research into phage-antibiotic combinations. Five publications, all from the past 5 years, described a total of 8 clinical cases of compassionate use of phage therapy against *A. baumannii* (septicaemia, osteomyelitis, surgical site infection, and 5 cases of ventilator-associated pneumonia), demonstrating varying degrees of success. In all of these cases, patients received, at least for a brief period of time, phages and antibiotics simultaneously. Therefore, it was difficult to quantify the precise contribution of phage therapy to the overall outcomes, and discriminate it from that of antibiotics. A further 18 articles reported the results of preclinical experiments using phages to treat infections in either rodents or wax moth larvae. The modelled infections included pneumonia, septicaemia, and wound infections, and a great majority demonstrated the bactericidal effect of phages *in vivo*. However, none of these studies assessed the activity of phage-antibiotic combinations. Lastly, 5 more studies did examine the therapeutic effects of phage-antibiotic combinations, and all of them reported at least one instance of synergy, primarily when carbapenem antibiotics or colistin were added to phages. Nevertheless, these studies used either *in vitro* platforms (tissue culture, liquid culture or biofilms) or wax moth models. Most importantly, we could not find in the literature instances where an exact mechanism of phage-antibiotic synergy against *A. baumannii* has been demonstrated in action.

Added value of this study

This work presents a preclinical study, using a mammalian model, that demonstrates that a phage-antibiotic combination has a superior bactericidal effect than each of these agents individually against severe *A. baumannii* infection. Notably, our findings explain the mechanism through which the combination of these two agents results in a superior bactericidal effect. We confirm that, even in complex *in vivo* systems, treatment with a capsule-targeting phage can reliably and repeatably induce bacterial evolution towards a phenotype that is phage-resistant but resensitised to antibiotics.

Implications of all evidence available

Phage therapy is becoming increasingly promising as a therapeutic strategy against *A. baumannii*. To maximise their therapeutic effect, however, the biology of clinically-relevant phages needs to be better understood. A clear knowledge of the bacterial receptor used by a phage, the mechanism of bacterial phage-resistance, and its associated trade-offs, can be leveraged as a clinical intervention. The emerging evidence supports the use of appropriate phage-antibiotic combinations as a better therapeutic strategy against this critical pathogen, warranting the design of clinical trials.

research, prevention and treatment of infectious diseases, it has also potentially contributed to worsening the problem of AMR.[1] The pandemic has, for example, exacerbated the issue of inappropriate prescription of antibiotics, and the saturation of the healthcare systems has correlated to an increase in healthcare-associated, multidrug-resistant bacterial infections.[1,2] In this context, *Acinetobacter baumannii* infections keep emerging as a leading cause of morbimortality in hospitalised patients.[3–6] The resilience, persistence, and AMR evolution of *A. baumannii* in hospital settings have been well documented,[7,8] with recent estimates suggesting almost half of *A. baumannii* clinical isolates are multidrug-resistant.[9] These precedents justify the declaration of *A. baumannii* as a critical priority for the research and development of new therapeutic strategies.[10]

In recent years, phage therapy has experienced a rebirth as a promising strategy against antimicrobial-resistant pathogens.[11] Preclinical studies of phage therapy in animal models of *A. baumannii* infection have demonstrated encouraging results.[12–16] Furthermore, clinical case studies have established the contribution of phage therapy in treating patients with severe *A. baumannii* septicaemia,[17] ventilator-associated pneumonia,[18,19] osteomyelitis,[20] and surgical site infections.[21] However, the interactions of *A. baumannii* with combinations of phage and traditional antimicrobial agents within an *in vivo* infection are currently understudied.

Therapeutic synergy occurs when the combined effect of two agents, in this case antimicrobials, is greater than the sum of their individual effects.[22] Phage-antibiotic synergy (PAS) was first detected *in vivo* against colibacillosis in broiler chicken,[23] but the term itself was coined three years later, upon observing how subinhibitory doses of antibiotics could increase the burst size of lytic phages *in vitro*.[24] The concept has since expanded with the discovery of more mechanisms through which antibiotics and phages potentiate each other's antibacterial effects.[11,25] A prime example is phage-resistance, whereby specific phages can push their hosts into evolutionary pathways that lead to phage-resistance at the cost of fitness trade-offs, including increased sensitivity to antibiotics.[26–28] Compared to other clinically relevant pathogens, however, PAS research against *A. baumannii* is limited,[29] with few studies exploring the combined effects of phages and

antibiotics, and primarily doing so *in vitro*.[30–32] More broadly, research into phage-resistance-mediated PAS should answer two key questions: (1) whether the *in vitro* identified mechanisms of phage-resistance repeatably occur within the substantially more complex and varied *in vivo* infections, and (2) if these do occur, whether *in vivo* combination treatments provide increased effectiveness compared to either treatment alone. Better understanding of these issues could provide important, new therapeutic insights.

Previously, we reported that phage øFG02 used the bacterial capsule of *A. baumannii* strain AB900 as its receptor.[33] In an effort to avoid killing by this phage, *A. baumannii* evolved loss-of-function mutations in genes of the K locus-responsible for capsule production and export.[33] The resultant capsule loss led to the sensitisation of phage-resistant mutants to beta-lactam antibiotics, the complement system, and alternative phages.[33]

The present work aimed to leverage our previous findings[33] and move them towards clinical translation. Here, we completed a preclinical study using a murine model of severe bacteraemia and tested whether a combined phage-antibiotic regime was superior to single-agent treatments. We confirmed that, similar to *in vitro*, the emergence of phage-resistance *in vivo* occurred via capsule loss, resulting in resensitisation to and greater killing by a beta-lactam antibiotic. Finally, we used an *in vitro* platform to confirm that a phage-antibiotic combination achieved synergistic, rather than just additive effects against *A. baumannii*. In summary, we validate the repeatability and predictability of phage-resistance evolution *in vivo* and enable a superior phage-antibiotic combination treatment against multidrug-resistant *A. baumannii* in a preclinical study.

Methods

Bacterial strains, phages, storage and culture conditions

Wild type *Acinetobacter baumannii* AB900 was previously described by Adams et al.[34] It is a clinical isolate originally obtained from a perineal wound of a patient at the Walter Reed National Military Medical Centre (USA), that harbours the resistance determinants *ampC* (cephalosporinase), $bla_{\text{OXA-51-like}}$ (carbapenemase), and *dhfrX* (dihydrofolate reductase), making it resistant to, among others, the third-generation cephalosporin ceftazidime (MIC $\geq$ 32 μg/ml).[34] AB900 contains the type-11 K locus (for capsule synthesis) and type-8 OC locus (for production of the outer membrane's lipooligosaccharide outer core).[35] The phage-resistant mutant strain of AB900 (øFG02-R AB900) obtained *in vitro* was characterised by Gordillo Altamirano et al.[33] Bacteria were cultured using lysogeny broth (LB) (Sigma-Aldrich), at 37 °C with aeration, supplemented with agar when required.

Phages øFG02 and øLK01 were originally isolated from raw sewage collected in Victoria, Australia, using the *A. baumannii* clinical strains AB900 and AB5075, respectively, as hosts of isolation.[33] A summary of the known characteristics of øFG02 is presented in Supplementary Table 1, including experimental confirmation of its lytic lifestyle in Supplementary Fig. 1.[33,36] Phage øLK01 has not been further characterised.[33] Phage stocks were amplified and purified using the Phage-on-Tap protocol[37] and stored at 4 °C.

Murine model of *A. baumannii* bacteraemia

The model has been previously described.[33] In summary, the experiments involved female, 6-to-10 weeks old, BALB/c mice, weighing at least 15 g; each animal was an experimental unit. In all cases, mice were randomly allocated to the different experimental groups. Late exponential phase bacterial inoculums of *A. baumannii* were prepared to the desired concentration depending on the experiment: 1×10^6 CFU for phage dosing, 2×10^6 CFU for ceftazidime dosing, and 5×10^6 CFU for both stages of the preclinical study. Inoculum size correlates with time of survival in untreated animals, with 5×10^6 CFU resulting in 100% mortality at 12 h, whereas 1×10^6 CFU enables survival to at least 24 h. In all cases, bacterial inoculums were calculated in 100 μl of PBS and mixed in a 1:1 ratio with 6% porcine stomach mucin (Sigma-Aldrich) in PBS, to enhance bacterial virulence,[38] for a total volume of 200 μl. Infection and treatments were all performed via intraperitoneal injection. All treatments were calculated for a volume of 200 μl, and the amount of injections received by each mouse was the same (using PBS if no other treatment was scheduled for a specific mouse at a specific timepoint).

Treatments for the phage dosing experiments (n = 4 mice per group; 8 total) were either a single dose of phage øFG02, at a multiplicity of infection (MOI) of 1, 1 h post infection (hpi) (once-a-day or q.d. group) or two doses, at 1 h and 12 hpi (twice-a-day or b.i.d group). In the ceftazidime dosing experiments (n = 3 per group; 12 total), treatments consisted of PBS (control) or a single dose of ceftazidime, delivered at 1 hpi, at either 12.5 mg/kg (low dose group), 25 mg/kg (medium dose group), or 50 mg/kg (high dose group), doses that correlate with standard veterinary and human treatments.[39,40] The first stage of the preclinical study (n = 4 per group; 16 total) involved treatments with either PBS (control), ceftazidime at 25 mg/kg every 8 h (antibiotic), phage øFG02 at a MOI of 1 as a single dose (phage) or the combination of the ceftazidime and phage treatments. The latter two treatments were used for the second, independent, stage of the preclinical study (n = 5 per group; 10 total).

The endpoints were set depending on the aim of each experiment. For phage and ceftazidime dosing

experiments, the endpoints were set at the end of the duration of action, i.e. right before the next dose in a clinical context would have been scheduled (24 h for phage dosing and 12 h for ceftazidime dosing). For the preclinical study, the endpoints were shortened considering the higher inoculum used. They were set at 12 h for the first stage and 16 h for the second stage. In all cases, a researcher blinded to the treatments received by the animals would follow them at regular intervals and, when needed, the programmed endpoints would be modified based upon animal wellbeing (humane endpoint).

At the endpoints, mice were euthanised by CO_2 asphyxiation. Blood and organs were collected, weighed and homogenised in PBS. Blood and organ suspensions were then serially diluted in PBS and the bacterial burden quantified by colony forming unit (CFU) counting, and normalised by organ weight, constituting our primary outcome. In mice that received phage treatment, the blood and organ suspensions were pelleted by centrifugation, and the supernatant serially diluted and plated with the soft overlay assay for plaque forming unit (PFU) quantification. Screening for phage-resistant mutants was performed as described below. Animals were housed at the Monash Animal Research Platform Facility, Monash University, with experiments starting after at least 48 h of acclimatization.

Screening for phage-resistant mutants

Bacterial colonies isolated from mice were patch-plated using sterile pipette tips onto fresh LB agar plates and individual wells of a microtiter plate filled with 200 μl of LB containing 10^6 PFU of phage øFG02. The agar plates were incubated overnight, while the microtiter plates were incubated for 16 h with OD_{600} measured at 15 min intervals. The growth curves of the putative phage-resistant mutants were compared to those of wild type AB900. Colonies with growth curves suggestive of phage-resistance underwent two rounds of single-colony purification starting from the previously prepared agar patch plates. Finally, the phenotype of each putative phage-resistant colony was confirmed by repeating the growth assay in liquid culture in the presence of phage, and the standard soft overlay assay. For the phage-resistant strains that underwent further characterisation, a final efficiency of plating assay was performed using a concentration of 10^9 PFU of øFG02 per plate, expecting a complete absence of plaques.

Isolation of bacterial genomic DNA, sequencing and variant calling

The GenElute™ Bacterial Genomic DNA Kit protocol (Sigma-Aldrich) was used for DNA isolation. Bacterial genomic DNA was tested for purity using a Nanodrop (NanoDrop Technologies), Qubit fluorometer (Life Technologies), and 1% agarose gel electrophoresis, then vacuum dried into a pellet for transport. Sequencing was performed using the Illumina® HiSeq 150 bp paired-end platform at the Genewiz® facilities (Suzhou, China).

The raw reads of each isolate's genome were examined using FastQC v0.11.9.[41] Raw reads were quality trimmed to remove adaptor sequences and reads of quality <20 in a sliding window of 4 bp using Trimmomatic v0.39.[42] Nucleotide variants were identified using "Snippy 4.3.6 - fast bacterial variant calling from NGS reads" (https://github.com/tseemann/snippy) with default settings, using the draft genome of wild type AB900 (NCBI Genbank accession number: JAAVKC010000001-JAAVKC010000043) as the reference. Snippy output files (*.csv) were then manually examined for the coverage and functional effect of variants. Synonymous, <20 read coverage and self-aligning variants (as described in Gordillo Altamirano et al.[33]) were removed from further analysis. Finally, frameshift variants were visualised in Integrative Genomics Viewer (IGV) v2.7.2[43] to examine the disruption of coding sequences.

Adsorption assay

Bacteria from overnight cultures and phages from pure lysates were mixed at a MOI of 0.01 (10^6 PFU/ml to 10^8 CFU/ml) in LB. The suspensions were incubated at 37 °C with aeration. At 0 and 20 min, samples of the suspensions were transferred into chloroform-saturated PBS, vortexed, and then centrifuged at 3500 × g for 3 min. The supernatant was diluted in PBS and plated in duplicate for quantification of free phage particles.

Scanning electron microscopy

A 20 μl droplet of 5 times-PBS washed AB900 bacterial suspension (~10^7 CFU/ml) was placed onto a fresh gold-coated silicon wafer (5 × 5 mm). The cells were allowed to settle for 5 min, followed by washing with PBS. Then, a 20 μl droplet of phage lysate (~10^9 PFU/ml) was added, incubated for 20 min, and washed with PBS. The wafer was then placed in 2.5% glutaraldehyde in PBS solution for 15 min, washed with deionized water and dehydrated by immersing in increasing concentrations of ethanol for 3 min each. Residual ethanol was removed with a critical point dryer EM CPD300 (Leica). The sample was mounted on a standard metal SEM stub and then coated with a ~5 nm thick gold layer using a sputter coater SCD 005 (BAL-TEC AG). The samples were examined within the FEG-SEM ThermoFisher Elstar G4 at an accelerating voltage of 2 kV, secondary electron mode, and a working distance of 3 mm, operating in immersion mode with the through lens detector. Images were colourised using the AKVIS Coloriage Software.

Serum killing assay

The working volume of human serum (Sigma-Aldrich, Australia) was divided in half, storing one half at 4°C and heat-inactivating the other (56°C for 30 min). In glass test tubes, aliquots of 5 ml of 50% serum (either active or heat-inactivated) in PBS were inoculated to 10^5 CFU/ml of bacteria in exponential growth phase. The tubes were thoroughly mixed and incubated. At the starting timepoint and at 60 min, samples from each tube were extracted to perform serial dilutions and CFU counts. *Escherichia coli* DH5-alpha was used as a control of serum activity (susceptible to human serum and resistant to heat-inactivated serum).

Antimicrobial susceptibility testing

Minimum inhibitory concentrations to ceftazidime and imipenem (Sigma-Aldrich) were assessed using the microbroth dilution protocol[44] and interpreted using the Clinical and Laboratory Standard Institute guidelines. *E. coli* strains ATCC 25922 and ATCC 35218 were used as quality controls for each batch of tests. The minimum bactericidal concentrations of ceftazidime were calculated using two methodologies (three technical replicates per strain, as detailed below), both starting from an incubated microbroth dilution test. First, 5 μl droplets from a range of wells (128 μg/ml to 2 μg/ml of ceftazidime, and the growth control) were streaked onto independent sections of a fresh (no antibiotic) Mueller Hinton agar plate, incubated overnight, and assessed for colony growth (two independent replicates). Alternatively, the microtiter plate was centrifuged (3500 × g for 10 min), the supernatant carefully aspirated and replaced with an equal volume of fresh Mueller Hinton broth, and the plate incubated for 16 h, at 37 °C, with continuous shaking, measuring the OD_{600} every 15 min. The resulting growth curves were analysed for bacterial growth (one replicate). Sensitivity to phage øLK01 was tested with the standard spot assay.

In vitro phage-antibiotic synergy experiments

The methodology, previously reported in,[45] was slightly modified here. AB900 was grown to exponential phase in LB, then adjusted to a concentration of 5×10^5 CFU/100 μl. Each well of the microtiter plate containing the checkerboard of phage øFG02 (range: 10^2–10^8 PFU/ml) and ceftazidime (range: 1–512 μg/ml) concentrations was inoculated with 5×10^5 CFU. The plate was incubated for 16 h, at 37°C, with continuous shaking, measuring the OD_{600} every 15 min.

Data representation and statistical analyses

Graphing and statistical analyses were performed using GraphPad Prism 7 (GraphPad Software, Inc.). For animal experiments with two groups, the variances of the outcome variables were compared to select the appropriate statistical tests. When variances were similar (bodyweight loss, proportion of phage-resistant mutants), a two-tailed t-test was used after applying the Shapiro-Wilk test to verify normal distribution; for unequal variances (bacterial and phage quantification), a two-tailed Mann-Whitney U-test was used instead. In experiments with multiple groups, comparison between groups were performed strictly following the pre-established hypotheses and tested with the Kruskal-Wallis test with Dunn's correction for multiple comparisons. Unless specified otherwise, all *in vitro* experiments were performed in triplicate, with at least two technical replicates each. For synograms, the raw OD data were first normalised with the negative control. Where necessary, the area under the bacterial growth curve (AUC) was calculated as well. To calculate the percent reduction in either OD or AUC, the following formula was used[45]: Reduction (%) = [(GrowthControl − Treatment)/GrowthControl] × 100. Two-way analysis of variance (ANOVA) was employed on interaction plots to analyse possible synergism between phage and antibiotics, after assessing the data for normality using the Shapiro-Wilk test. For all statistical analyses, the threshold value of two-tailed $p < 0.05$ was used for statistical significance.

Ethics statement

All protocols involving animals were reviewed and approved by the AMREP (Alfred Medical Research and Education Precinct) Animal Ethics Committee (Project ID: E/1781/2018/M) and complied with the National Health and Medical Research Council guidelines. The reporting of animal research in this study complied with the ARRIVE (Animal Research: Reporting of *In Vivo* Experiments) guidelines.[46]

Role of funders

The funders of the study did not have any role in the study design; in the collection, analysis, and interpretation of data; in the writing of the report; or in the decision to submit the paper for publication.

Results

The combination of phage øFG02 with ceftazidime is superior to single-agent treatments against *Acinetobacter baumannii* bacteraemia

Using an established murine model of *A. baumannii* bacteraemia,[33] we first set out to validate the ideal dosage and administration timings for the phage and antibiotic treatments. We had previously determined a starting bacterial inoculum of mid-10^6 CFU per mouse consistently produced a 100% lethality rate without effective treatment at 12 h,[33] mirroring the severity of *A. baumannii* bacteraemia in humans.[47,48] First we compared the effect of once-a-day (q.d.) versus twice-a-day

(b.i.d) intraperitoneal (IP) administration of phages on animal bodyweight and average bacterial and phage counts at 24 hpi. To ensure mouse survival to 24 h, the starting inoculum was reduced to low-10^6 CFU/mouse; and treatment with phage øFG02 at a multiplicity of infection (MOI) of 1 was administered at either 1 h-only or at 1 h and 12 hpi. We found that b.i.d. phage treatment did not provide any significant benefits compared to q.d. administration (Supplementary Fig. 2). Next, we investigated whether there was any significant difference in antibacterial effect between varying doses of the beta-lactam ceftazidime, representing low (12.5 mg/kg), medium (25 mg/kg) and high (50 mg/kg) doses in animals and adult humans.[39,40] Mice were infected with low-10^6 CFU/mouse of *A. baumannii* and the antibiotic administered as a single dose 1 hpi, with an endpoint at 12 h. Consistent with AB900's resistance to ceftazidime *in vitro*, we observed only a slight reduction in the bacterial burden in the animals at 12 h, with no significant differences observed between the various doses of ceftazidime (Supplementary Fig. 3). These data provided the necessary phage and antibiotic parameters for our subsequent treatment experiments.

We then carried out a two-staged preclinical study comparing four treatments against *A. baumannii* AB900 bacteraemia (Figure 1a,b). In the first stage, groups of mice ($n = 4$) were treated with either (i) PBS as a negative control; (ii) 25 mg/kg ceftazidime every 8 h; (iii) phage øFG02 at a MOI of 1 as a single dose; or iv) the combination of the ceftazidime and phage treatments. The main measured outcome was the average bacterial burden from four body sites per mouse (blood, liver, kidney, and spleen). Mice were euthanised at 11 hpi when humane endpoints were reached in the negative control and antibiotic-only groups. Compared to the other groups, combination treatment reduced bacterial density by 3.7, 2.9, and 1.4 log, against the control, antibiotic-only, and phage-only groups, respectively (Figure 1c); with data analysis in individual organs showing the same trend (Supplementary Fig. 4). While the combination treatment showed the strongest bactericidal effect, it did not achieve statistical significance when compared to the phage-only treatment (Figure 1c) (Kruskal-Wallis test with Dunn's correction for multiple comparisons, $p = 0.003$ vs control, $p = 0.0428$ vs antibiotic-only, $p = 0.851$ vs phage-only). Notably, there was no difference in the numbers of active phage particles or phage-resistant bacterial colonies retrieved from the mice receiving either phage-only or combination treatment (Mann-Whitney U-test, $p = 0.2$ and $p = 0.08$, respectively; two-tailed) (Figure 1d,e).

In the second, independent, stage of the study ($n = 5$ per group), we excluded the negative control and antibiotic-only groups, allowing the extension of the endpoint to 16 h. Here we observed that the combination treatment achieved a sustained suppression of the bacterial burden, whereas the phage-only group experienced a resurgence in bacterial burden, for a final 1.6 log difference (median: 8.38×10^7 vs 2.08×10^6 CFU/g of tissue; Mann-Whitney U-test; $p = 0.03$; two-tailed) (Figure 1f). The higher bacterial load in the phage-only group was correlated to higher phage quantities (median: 1.35×10^8 vs 1.08×10^7 PFU/g of tissue; Mann-Whitney U-test; $p = 0.0159$; two-tailed) (Figure 1g), and both groups had a similar proportion of phage-resistant mutants (unpaired t-test; $p = 0.29$; two-tailed) (Figure 1h). In summary, our preclinical study demonstrated greater efficacy with the combination of ceftazidime and phage øFG02 compared to either antibiotic-only or phage-only approaches against *A. baumannii* bloodstream infection.

Phage-resistant *A. baumannii* mutants emerge *in vivo* via a repeatable evolutionary pathway that leads to antimicrobial resensitisation

We hypothesised that the success of the combination therapy *in vivo* was due to the emergence of phage-resistant mutants exhibiting antimicrobial resensitisation.[33] To explore this hypothesis, we screened for phage-resistant mutants as an outcome measure from all phage or combination treated mice across all experiments (Figure 1e,h, Supplementary Fig. 2d). A minimum of 15 bacterial colonies per mouse were randomly selected, from different body sites. Following two rounds of single-colony purification, the sensitivity of these colonies to phage øFG02 was assessed with growth curves and the standard soft agar overlay assay. In total, phage-resistant colonies were isolated from 24 out of 25 mice (96%). The frequency of phage-resistance emergence was not necessarily comparable between mice across different experiments, ranging from as little as 5% of colonies per mouse up to as many as 94% (Supplementary Fig. 5). This range was likely due to variations in starting inoculums, number of phage doses, and length of follow-up. We did however observe phage-resistant isolates within all four organs. This result confirmed that *A. baumannii* AB900 can become resistant to phage øFG02 *in vivo*.

In vitro resistance to phage øFG02 in AB900 had previously been determined to occur via loss-of-function mutations in genes associated with capsule production.[33] We next sought to verify if the mechanisms of phage resistance in our *in vivo* derived isolates were the same as those that evolved *in vitro*. We randomly selected one phage-resistant isolate from 11 animals (Supplementary Fig. 5), reconfirmed their phage-resistant phenotype with an efficiency of plating assay using 10^9 PFU of øFG02 per plate (Supplementary Fig. 6), and prepared them for whole genome sequencing. We compared the genomes of these strains to the wild type's (NCBI BioProject accession number SAMN14483301) to identify mutations. Similar to that observed *in vitro*,[33] each *in vivo* phage-resistant isolate

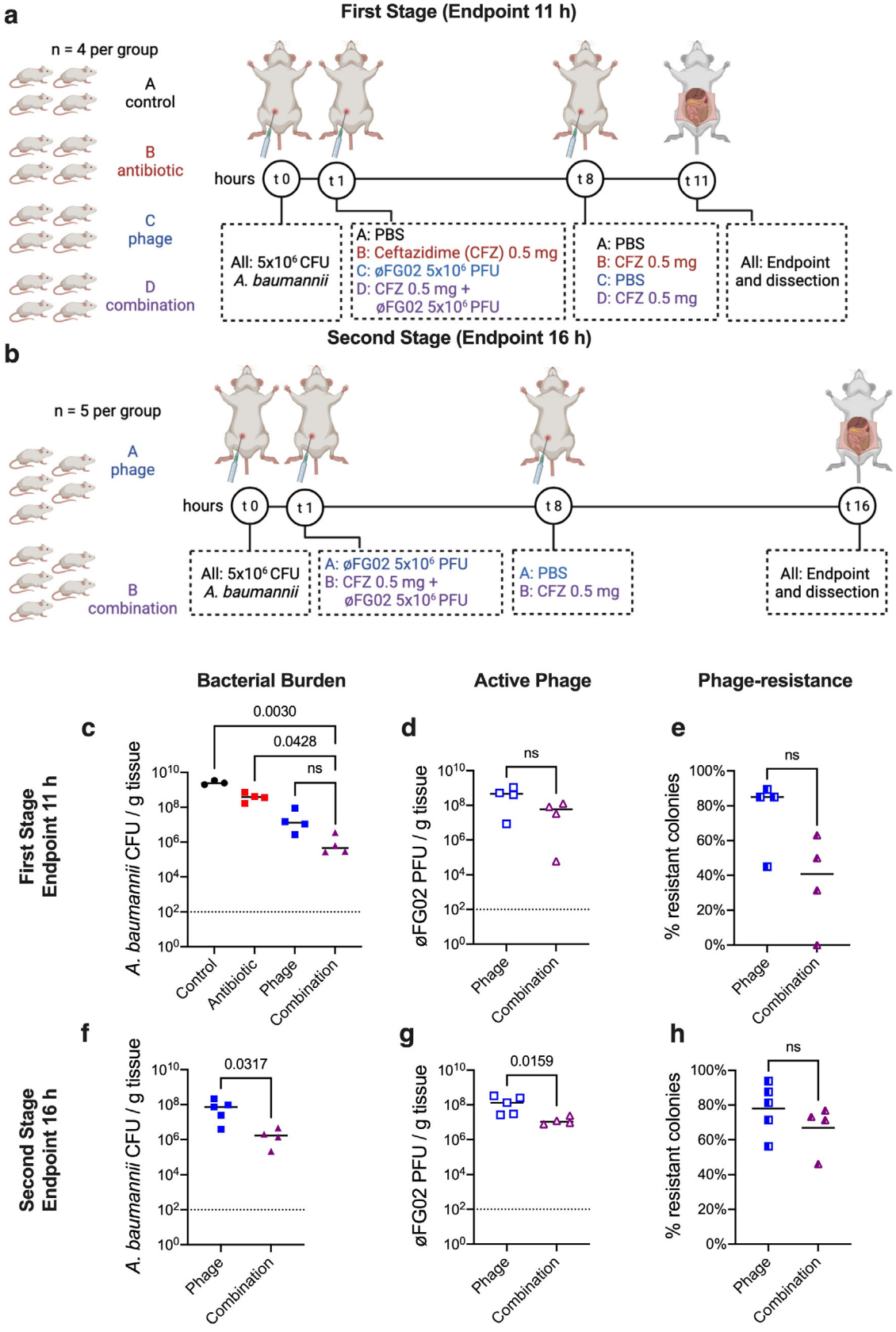
a
First Stage (Endpoint 11 h)
n = 4 per group
A control
B antibiotic
C phage
D combination
hours
t 0
t 1
t 8
t 11
All: 5x10⁶ CFU A. baumannii
A: PBS
B: Ceftazidime (CFZ) 0.5 mg
C: øFG02 5x10⁶ PFU
D: CFZ 0.5 mg + øFG02 5x10⁶ PFU
A: PBS
B: CFZ 0.5 mg
C: PBS
D: CFZ 0.5 mg
All: Endpoint and dissection
b
Second Stage (Endpoint 16 h)
n = 5 per group
A phage
B combination
hours
t 0
t 1
t 8
t 16
All: 5x10⁶ CFU A. baumannii
A: øFG02 5x10⁶ PFU
B: CFZ 0.5 mg + øFG02 5x10⁶ PFU
A: PBS
B: CFZ 0.5 mg
All: Endpoint and dissection
Bacterial Burden
Active Phage
Phage-resistance
First Stage Endpoint 11 h
Second Stage Endpoint 16 h
c
d
e
f
g
h
A. baumannii CFU / g tissue
øFG02 PFU / g tissue
% resistant colonies
0.0030
0.0428
ns
0.0317
0.0159
Control
Antibiotic
Phage
Combination

Isolate	Tissue of isolation	Treatment received	Mutation Type	Affected Gene	nt Position	Effect	Product and function
1	Kidney	Phage only	Insertion (1 nt)	*gtr29*	877/1041	Frameshift	Glycosyltransferase 29: elongates the K unit adding sugars
2	Blood	Phage only	Substitution (1 nt)	*tle*	401/1134	Gly134Asp	Talose epimerase: synthesis of complex sugars for the K unit
3	Spleen	Phage only	Deletion (20 nt)	*gtr29*	865/1041	Frameshift	Glycosyltransferase 29: elongates the K unit adding sugars
4	Liver	Phage only	Deletion (3 nt)	*gtr29*	610/1041	Tyr204del	Glycosyltransferase 29: elongates the K unit adding sugars
5	Kidney	Phage only	Insertion (1 nt)	*gpi*	163/1671	Frameshift	Glucose-6-phosphate isomerase: synthesis of simple sugars for the K unit
6	Spleen	Phage only	Insertion (1 nt)	*wzx*	254/1269	Frameshift	Oligosaccharide flippase: translocates the K unit into the periplasm
7	Blood	Phage only	Deletion (1 nt)	*gtr29*	819/1041	Frameshift	Glycosyltransferase 29: elongates the K unit adding sugars
8	Spleen	Phage only	Deletion (1 nt)	*gtr29*	193/1041	Frameshift	Glycosyltransferase 29: elongates the K unit adding sugars
9	Liver	Phage and antibiotic	Deletion (3 nt)	*gtr29*	212/1041	Frameshift	Glycosyltransferase 29: elongates the K unit adding sugars
10	Liver	Phage and antibiotic	Deletion (3 nt)	*gtr29*	610/1041	Tyr204del	Glycosyltransferase 29: elongates the K unit adding sugars
11	Liver	Phage and antibiotic	Insertion (1 nt)	*pgm*	979/1371	Frameshift	Phosphoglucomutase: synthesis of simple sugar for the K unit

***Table 1*: Mutations harboured by the *in vivo*-obtained phage-resistant AB900 isolates. Whole genomic DNA short-read sequenced, assembled and compared to wild type AB900. All affected genes are in the K locus.**
nt: nucleotide.

harboured mutations in genes of the K locus (Table 1).[35,49] Interestingly, the affected gene in 7 of the 11 isolates was *gtr29*, a glycosyltransferase previously found to have lost its function *in vitro*.[33] Furthermore, two of these strains had the same mutation, a 3-nucleotide deletion resulting in the loss of the tyrosine residue at position 204. The remaining isolates contained mutations in genes involved in the production of simple and complex sugars used for the capsule (*tle:* talose epimerase, *gpi*: glucose-6-phosphate isomerase, and *pgm:* phosphoglucomutase), and in the export of the capsule (K) subunits into the periplasm (*wzx*: oligosaccharide flippase) (Figure 2a).[50] We next confirmed that these mutations inhibited the adsorption of phage øFG02 (Figure 2b). Over a period of 20 min, more than 99% of øFG02 particles were able to attach to their wild type

Figure 1. Preclinical study of phage-antibiotic combination therapy against *A. baumannii* bacteraemia. a and b: Experimental design for the two-staged preclinical study. The experiments began with the intraperitoneal injection of 5×10^6 CFU/mouse of *A. baumannii* AB900. Treatments were also delivered intraperitoneally, at 1 h and 8 h post-infection. At the endpoints of 11 h or 16 h, blood, liver, kidney and spleen from each mouse were obtained for bacterial and phage quantification. c to e: Results of the first stage of the study, endpoint at 11 h, comparing control (black), antibiotic-only (red), phage-only (blue), and combined (purple) therapies. f to h: Results of the second stage of the study, endpoint at 16 h, comparing phage-only (blue), and combined (purple) therapies. Average bacterial burdens from 4 body sites (c and f) are represented by solid symbols, average active phage counts (d and g) by outline-only symbols, and proportion of phage-resistant colonies (e and h) by shaded symbols. Each data point represents one mouse, bars are medians and dotted lines represent the assays' detection limit. Statistical analysis was performed using the Kruskal-Wallis test with Dunn's correction for multiple comparisons (c), Mann-Whitney U-test (d, e f, and g), and unpaired t-test (h). Data by organ from panels c-d and f-g available in Supplementary Fig. 4. Two data points have been excluded due to suspected incorrect administration (intraintestinal, intramuscular or subdermal) of either inoculum or phage treatment. In the missing data point from c (control group) suspected incorrect administration of the inoculum lead to no infection being established, noticed by undetectable levels of bacteria at the endpoint. In the missing data point from f-h (combination group), suspected incorrect administration of the phage treatment led to the animal reaching the endpoint at 12 h instead of 16 h, alongside undetectable levels of phage from all organs. ns: not significant.

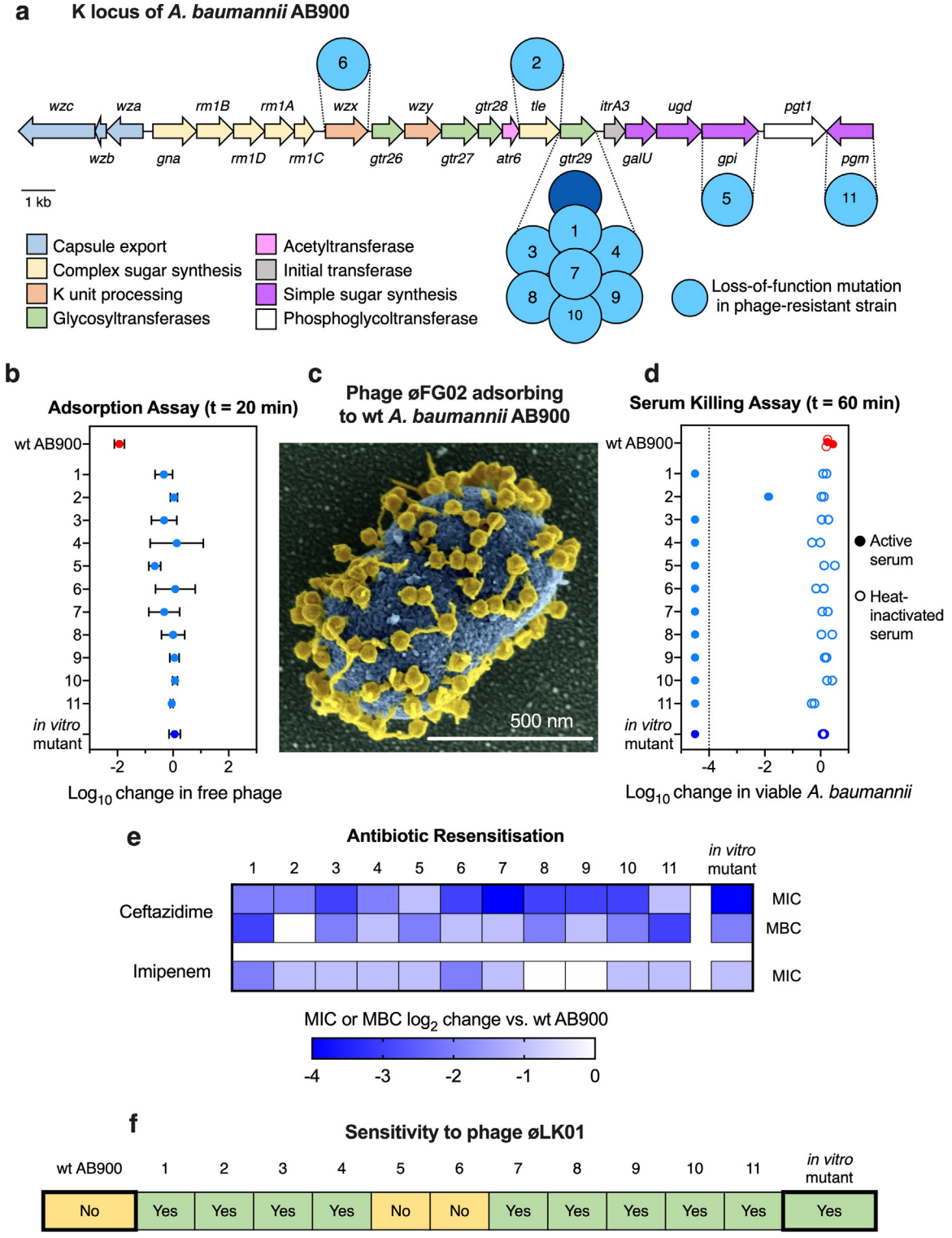

Figure 2. The mechanism and trade-offs of phage-resistance in *A. baumannii* AB900 are repeatable *in vivo*. a: Schematic representation of the genes of the K locus of AB900, based on.[49,50] The high-level functions of their products are colour-coded; the dark blue circle represents the mutated gene in the previously described *in vitro*-obtained phage-resistant mutant,[33] while the light blue circles represent the mutated genes in the *in vivo*-obtained phage-resistant isolates from this study (designated with the numbers

host, AB900 (also visualised with scanning electron microscopy in Figure 2c); however, øFG02 particles did not adsorb to any of the 11 *in vivo* phage-resistant strains. Finally, we tested if we could recapitulate the phenomenon of antimicrobial resensitisation in these strains, using human serum, two antibiotics and one alternative phage.[33] In a human serum killing assay, we observed that 10 of the phage-resistant mutants were eradicated by human serum after only 60 min of coincubation, with this bactericidal effect disappearing if heat-inactivation of the serum was performed beforehand (Figure 2d). Next, we used the microbroth dilution method, and a subsequent subculture into fresh media, to determine the minimum inhibitory (MIC) and bactericidal (MBC) concentrations, respectively, of ceftazidime and imipenem (Figure 2e, Supplementary Table 2, and Supplementary Figs. 7 and 8). Compared to wild type AB900, all 11 phage-resistant strains had reductions in the MIC of ceftazidime, 10 of them carried a corresponding reduction in the MBC of the antibiotic, and 9 had a reduced MIC to imipenem. Likewise, 9 out of 11 strains had become susceptible to øLK01, a phage to which wildtype AB900 is resistant (Figure 2f). Taken together, these results suggest that inhibition of phage adsorption through disruption of capsule synthesis is a repeatable mechanism of resistance used by *A. baumannii* AB900 against phage øFG02; and it consistently results in the trade-off of antimicrobial resensitisation. These findings explain the success of combination therapy in our preclinical experiments, supporting our hypothesis.

The combined effect of ceftazidime and phage øFG02 against *A. baumannii* AB900 is synergistic

The results of our preclinical study suggest that ceftazidime and øFG02 achieve at least an additive effect when combined against *A. baumannii* AB900. A hypothesis of phage-antibiotic synergy (PAS) could be made, after corroborating that resensitisation to ceftazidime is a repeatable effect of resistance to øFG02. However, *in vivo* confirmation of antimicrobial synergy is notoriously fickle,[51] and most *in vitro* and computational platforms that test for synergy may not cater for the unique biology of phages.[22,52] Here, we tested our hypothesis using the synogram, an *in vitro* model based on the gold standard time-kill curve[53] and the traditional checkerboard assay, and validated for phage-antibiotic combinations.[45] With the synogram, we assessed the antimicrobial effect of ceftazidime at concentrations of 1 to 512 μg/ml and phage øFG02 at concentrations of 10^2 to 10^8 PFU/ml. Varying combinations of both agents were assessed and a no-treatment control was used. The measured outcomes were the size of the bacterial population at 16 h (Figure 3a) and the area under the bacterial growth curve (Figure 3b). By analysing individual wells of the synogram, we observed that all phage concentrations eventually lead to the emergence of phage-resistance, and most importantly, that even subinhibitory doses of phage and ceftazidime achieved sustained bacterial suppression when used in combination (Figure 3c). Finally, we used these data to construct interaction plots (Figure 3d,e) comparing the endpoint effect of ceftazidime when it was used with and without phage øFG02. The plots demonstrate that the addition of øFG02 increased the bactericidal effect of ceftazidime by more than the phage's bactericidal effect alone (divergent lines in the plots, Figure 3e) (two-way ANOVA; "phage" factor; $p = 0.0264$ for CFZ 1 μg/ml with øFG02 10^6 PFU/ml; and $p = 0.0001$ for CFZ 1 μg/ml with øFG02 10^7 PFU/ml; CFZ 2 μg/ml with øFG02 10^6 PFU/ml; and CFZ 2 μg/ml with øFG02 10^7 PFU/ml). As such, we could confirm the existence of synergy between ceftazidime and øFG02 against *A. baumannii* AB900, at least *in vitro*.

Discussion

Clinical translation of new therapeutic strategies against *A. baumannii*, although extremely necessary, can be challenging. Here, we have advanced the translation of a phage-antibiotic combination strategy taking advantage of the knowledge of phage receptor[54] and the mechanism for the emergence of phage-resistance[33] in *A. baumannii*. In this study, we have successfully demonstrated that the combination of ceftazidime with phage

on Table 1); scale bar = 1 kb. b: Adsorption assay. Log_{10} reduction in free phage titres 20 min after mixing phages and hosts. øFG02 was mixed with either wild type (red), *in vitro* phage-resistant (blue), or each of the 11 *in vivo*-obtained phage-resistant isolates (light blue). Phages only adsorb to wild type AB900. One-way ANOVA comparison between wild type AB900 and each of the phage-resistant isolates; $p < 0.05$ for all cases; two-tailed; all other comparisons were non-significant. Data are mean ± s.e.m. ($n = 3$). c: Coloured scanning electron microscopy image of øFG02 particles (yellow) adsorbing to the capsule of wild type AB900 (blue). Scale bar = 500 nm. d: Human serum killing assay. Log_{10} reduction in viable *A. baumannii* after 60 min of incubation in 50% active (solid symbols) or heat-inactivated (outline-only symbols) human serum in PBS. Dotted line represents the assay's limit of detection. ($n = 2$ for each of the conditions). e: Antibiotic resensitisation in phage-resistant isolates. The minimum inhibitory concentrations (MIC) of ceftazidime and imipenem were measured using the microbroth dilution method. For ceftazidime, the minimum bactericidal concentration (MBC) was measured by subculturing wells of the microbroth dilution tests into fresh media without antibiotic. The median ($n = 3$) of the log_2 reduction in MIC and MBC of phage-resistant strains, compared to the wild type, is represented by the intensity of the blue shading of the cells. Raw data values and methods are available in Supplementary Table 2, and Supplementary Figs. 7 and 8. f: Changes in the phage sensitivity pattern. The infectivity of phage øLK01 was tested in each of the 11 strains, with nine being susceptible (green, as in the *in vitro* mutant) and two being resistant (yellow, as in wild type AB900)

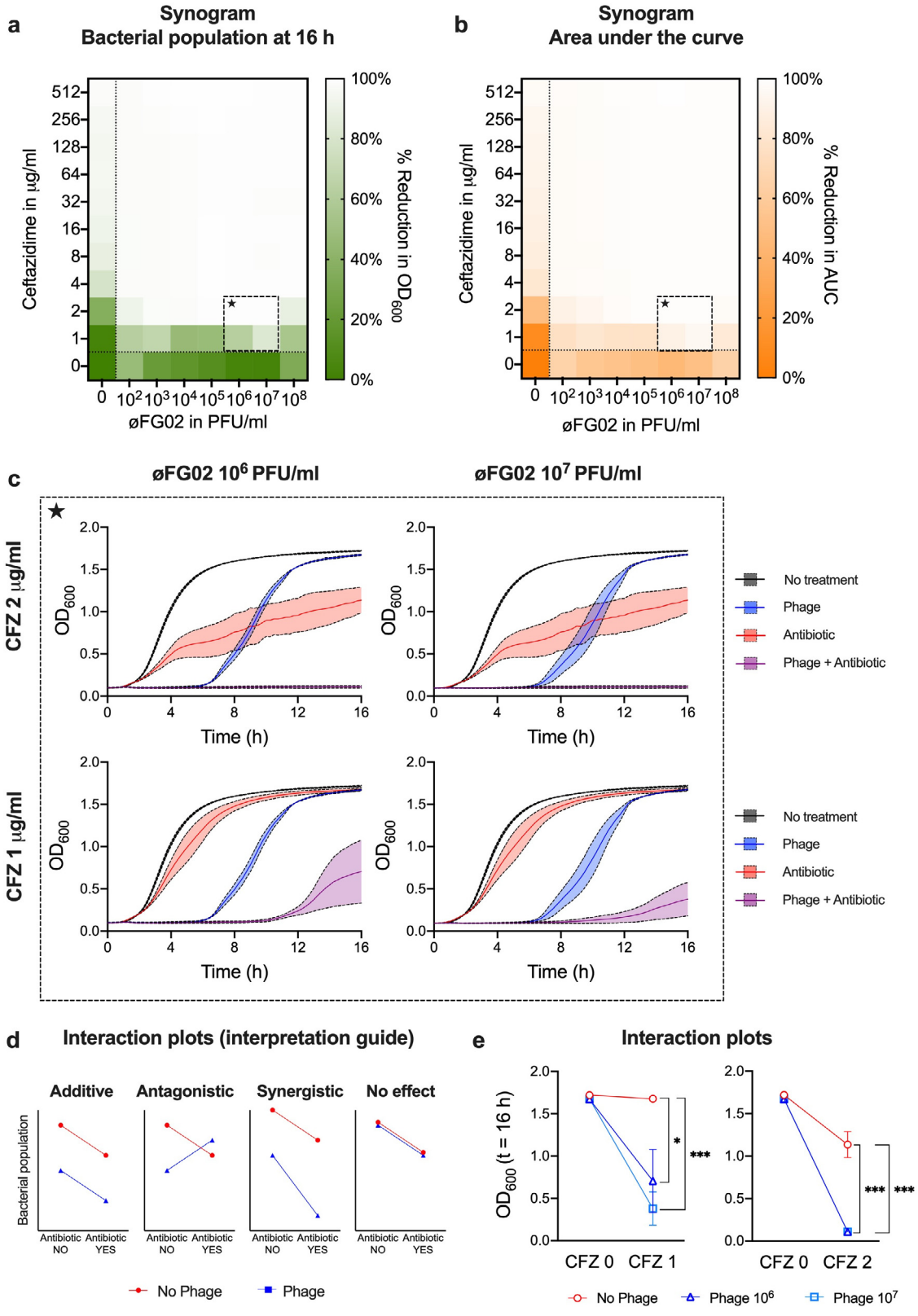
a
Synogram
Bacterial population at 16 h
Ceftazidime in µg/ml
512
256
128
64
32
16
8
4
2
1
0
0 10² 10³ 10⁴ 10⁵ 10⁶ 10⁷ 10⁸
øFG02 in PFU/ml
100%
80%
60%
40%
20%
0%
% Reduction in OD600
b
Synogram
Area under the curve
Ceftazidime in µg/ml
øFG02 in PFU/ml
% Reduction in AUC
c
øFG02 10⁶ PFU/ml
øFG02 10⁷ PFU/ml
CFZ 2 µg/ml
CFZ 1 µg/ml
OD600
Time (h)
No treatment
Phage
Antibiotic
Phage + Antibiotic
d
Interaction plots (interpretation guide)
Additive
Antagonistic
Synergistic
No effect
Bacterial population
Antibiotic NO
Antibiotic YES
No Phage
Phage
e
Interaction plots
OD600 (t = 16 h)
CFZ 0
CFZ 1
CFZ 2
*
***
No Phage
Phage 10⁶
Phage 10⁷

øFG02 is better than each agent individually in a preclinical model of bacteraemia. The superiority of this approach can be explained by understanding the interactions between phages, their bacterial and mammalian hosts, and antibiotics.

Previous *in vitro* findings illustrated the emergence of AB900 resistance against phage øFG02 through capsule loss, resulting in decreased fitness and antimicrobial resensitisation.[33] Here, we also tackled a logical subsequent question: whether the evolution of similar mutations would occur in a complex *in vivo* environment.[55] This work provides evidence that for this phage-host pair, this mechanism of bacterial phage-resistance *in vivo* is repeatable and predictable. Phage-resistant mutants emerged in 24 out of 25 animals receiving phage øFG02, either alone or in combination, and all of the 11 randomly selected resistant isolates contained mutations in genes of the K locus, resulting in abolition of phage adsorption. Most importantly, all phage-resistant mutants showed increased sensitivity to ceftazidime, with 9 of the 11 becoming either vulnerable to an alternative phage, øLK01, or more sensitive to imipenem. Of note, populations of 10 of the 11 strains could be eradicated by 60 min of incubation in human serum, although this finding might not have contributed to the results in the murine models given the poor complement activity of mouse sera.[56] In any case, our findings support a model in which the combination treatment acts as a staggered "one-two punch", with initial phage dosing partially killing the bacterial population and driving the emergence of phage-resistant variants, which are then resensitised to and killed by the antibiotic.

Phages that induce repeatable and predictable phage-resistant phenotypes in their hosts have been previously described.[57,58] These phages can certainly be clinically useful, but it is worth remembering that not all phage-host pairs will behave in the same way.[59–61] Interestingly, while the locus of loss-of-function mutations in our phage-resistant strains was repeatable, and mutations primarily clustered in genes involved in the early steps of capsule production,[62] the specific genes, types of mutations and nucleotide positions were not all the same, suggesting a degree of flexibility and diversity in the variants. It is entirely possible for some of these variants to differ in other fitness trade-offs. Our findings do not completely exclude the chance of alternative, unrelated, mechanisms of resistance against øFG02. However, they do suggest that, if possible, those mechanisms might require a more complicated evolutionary route to emerge, or are present in lower proportions, arguably making them irrelevant in the clinical setting. Finally, and although unseen here, another possibility is the occurrence of subsequent compensatory mutations or reversion to the wild type phenotype.

During optimisation experiments, we observed that once-a-day (q.d.) and twice-a-day (b.i.d) phage administration regimes appeared to be equivalent. Namely, we observed no differences in neither their antibacterial effect, phage levels, or emergence rate of phage-resistance. While these findings successfully guided the design of our preclinical study, deeper research into the pharmacology of phage therapy is certainly warranted. It is becoming increasingly apparent that the interactions between phages and eukaryotic cells also need to be accounted for when planning phage therapy regimes, as factors such as mammalian cell type and phage size can influence cellular uptake of phage and thus, phage bioavailability.[63]

While the resulting *in vivo* model reflects the severity of *A. baumannii* bacteraemia in humans, our analyses stemming from it still present some limitations. Firstly, by sampling only four body sites (blood, liver, kidney, and spleen), we could possibly be missing body sites that act as bacterial reservoirs, or where phages do not reach in sufficient quantity to trigger the emergence of phage-resistant variants. Second, the arguably short endpoint of 16 h makes it hard to establish conclusions on the long-term sustainability of the combined therapy, and the model was not amenable to a prolonged survival experiment. Third, the use of the intraperitoneal administration route, which may not have a perfect correlation with the intravenous route used in humans, could influence phage bioavailability and effectiveness at specific body sites.[64]

A further limitation is that our results are restricted to the antibiotic ceftazidime and phage øFG02. However, we hypothesise that similar results could be obtained with other phages that target *A. baumannii*'s capsule, thus inducing capsule loss upon emergence of

Figure 3. Synergy between ceftazidime (CFZ) and phage øFG02 *in vitro*. a and b: Synograms of ceftazidime (CFZ) (1 to 512 μg/ml, rows) and phage øFG02 (10^2 to 10^8 PFU/ml, columns); wells below or to the left of the dotted lines contained single treatment of phage or antibiotic, respectively; the bottom left well served as a no-treatment control; the mean reduction in bacterial density at the endpoint (t = 16 h; $n = 3$) is colour coded by the shades of green (a), while the reduction in the area under the curve (AUC) is in orange (b). Wells of combination treatment that are analysed in panel c are delineated with the dashed squares containing a star. c: Growth curves of *A. baumannii* AB900 with varying doses of phage øFG02 (blue), ceftazidime (red), both (purple), or neither (black). Data are mean ± s.e.m ($n = 3$). Curves show how the combination of subinhibitory doses of phage and antibiotic achieves effective bacterial suppression. d and e: Interaction plots of the antimicrobial effects of ceftazidime and phage øFG02 suggest the existence of synergy (interpretation key presented in d, as per[45]: additive effect would result in parallel lines, antagonism in convergent lines, synergy in divergent lines, no effect in superimposed lines). Data are mean ± s.e.m ($n = 3$). Two-way ANOVA for statistical analysis; "phage" factor; * $p < 0.05$; ***$p = 0.0001$. OD_{600}=optical density at 600 nm.

phage-resistance. It could even be possible for similar phenomena to emerge with other capsulated pathogens, as suggested by preliminary observations in *Klebsiella pneumoniae*[65] and *Pseudomonas aeruginosa*.[66] A final caveat regarding phage øFG02 is that, despite multiple attempts,[33] its genome remains unsequenced. Here we have used a phenotypic assay[36] to rule out lysogenic behaviour in øFG02 (Supplementary Fig. 1) but it would be advisable to obtain sequencing data before using it in a clinical setting.

Previous studies have shown evidence of synergy between *A. baumannii*-specific phages and the beta-lactams imipenem[32] and meropenem.[30,32] as well as the outer-membrane disrupting agent colistin[30,31,67] either *in vitro* or using the *Galleria mellonella* larvae system. However, our study demonstrates the superiority of a phage-antibiotic combination using a mammalian model, furthering its translational potential. Furthermore, we confirmed that, at least *in vitro*, ceftazidime and phage øFG02 achieve synergistic, instead of just additive, effects.

Further research in the field will surely lead to the discovery of innovative uses of combination therapies using phages, rather than proposing phages as a substitute to antibiotics.[11] As an example, in the reviewed clinical cases of phage therapy use against *A. baumannii,* the patients received-at least for a brief period-phages and antibiotics simultaneously[17–21]; and in at least one of those cases, therapeutic synergy may have contributed to the patient's favourable outcome.[17] In fact, it is reasonable to believe that the translation of phage therapy into widespread clinical use could be spearheaded by the use of phage-antibiotic combinations. In this study, we have provided insights that further advance the development of combination-based therapeutic approaches using phages against the top priority pathogen *A. baumannii*.

Contributors

F.G.A., A.Y.P. and J.J.B. conceived the study. F.G.A., and X.K. performed *in vivo* experiments. F.G.A. performed characterisation of phage-resistant mutants and *in vitro* synergy testing. D.S. led the bioinformatic analyses, with F.G.A. providing further input. D.K. performed scanning electron microscopy. A.Y.P. and J.J.B. provided resources for experimental work. A.Y.P. and J.J.B. supervised and funded the project. F.G.A. wrote the original draft, with J.J.B. providing further feedback and editing. Underlying data has been verified by F.G.A., X.K., and J.J.B. (*in vivo* experiments), F.G.A., D.S., and J.J.B. (bioinformatics), and F.G.A., and J.J.B. (*in vitro* experiments). All authors were involved in reviewing and editing the final manuscript.

Data sharing statement

Sequencing data are available with the NCBI BioProject accession number: PRJNA608808. This work did not involve the creation of novel code for bioinformatics analyses. All the used software is freely accessible and appropriately referenced. Raw data from all experiments are available upon reasonable request.

Declaration of interests

The authors declare no competing interests.

Acknowledgements

Fernando L. Gordillo Altamirano acknowledges the support from Monash University through the Monash Postgraduate Research Scholarships that funded his doctoral studies, and the Monash Postgraduate Publication Award (Round 1, 2021). Anton Y. Peleg is supported by a National Health and Medical Research Council Practitioner Fellowship (APP1117940). This work, including the efforts of Jeremy J. Barr, was funded by the National Health and Medical Research Council (NHMRC: 1156588), Perpetual Trustees Australia award (2018HIG00007), and Frontier Health Medical Research (RFRHPI000017). We thank the Monash Ramaciotti Cryo-EM platform for the use of the facility and Alex de Marco for granting access to the SEM; as well as the MASSIVE high performance computing facility (www.massive.org.au) for providing us cluster time for data analysis. We also thank Dr María José Fierro for her comments on the structure and readability of the manuscript. Figure 1a,b was made using BioRender (biorender.com).

Supplementary materials

Supplementary material associated with this article can be found in the online version at doi:10.1016/j.ebiom.2022.104045.

References

1 Getahun H, Smith I, Trivedi K, Paulin S, Balkhy HH. Tackling antimicrobial resistance in the COVID-19 pandemic. *Bull World Health Organ*. 2020;98:442.442A.
2 Ruiz J. Enhanced antibiotic resistance as a collateral COVID-19 pandemic effect? *J Hosp Infect*. 2021;107:114–115.
3 Lescure F-X, Bouadma L, Nguyen D, et al. Clinical and virological data of the first cases of COVID-19 in Europe: a case series. *Lancet Infect Dis*. 2020;20:697–706.
4 Gottesman T, Fedorowsky R, Yerushalmi R, Lellouche J, Nutman A. An outbreak of carbapenem-resistant *Acinetobacter baumannii* in a COVID-19 dedicated hospital. *Infect Prev Pract*. 2021;3: 100113.
5 Sharifipour E, Shams S, Esmkhani M, et al. Evaluation of bacterial co-infections of the respiratory tract in COVID-19 patients admitted to ICU. *BMC Infect Dis*. 2020;20:646.
6 Kuehn BM. Drug-resistant bacteria outbreak linked to COVID-19 patient surge. *JAMA*. 2021;325:335.
7 Hawkey J, Ascher DB, Judd LM, et al. Evolution of carbapenem resistance in *Acinetobacter baumannii* during a prolonged infection. *Microb Genom*. 2018;4: e000165.
8 Peleg AY, Seifert H, Paterson DL. *Acinetobacter baumannii*: emergence of a successful pathogen. *Clin Microbiol Rev*. 2008;21:538–582.
9 Weiner-Lastinger LM, Abner S, Edwards JR, et al. Antimicrobial-resistant pathogens associated with adult healthcare-associated

infections: summary of data reported to the national healthcare safety network, 2015–2017. *Infect Control Hosp Epidemiol*. 2020;41:1–18.
10 World Health Organization. Global Priority List of Antibiotic-Resistant Bacteria to Guide Research, Discovery, and Development of New Antibiotics. [Internet]. Geneva; Switzerland: World Health Organization. [2017; cited January 2021]. Available from: https://www.who.int/medicines/publications/WHO-PPL-Short_Summary_25Feb-ET_NM_WHO.pdf?ua=1.
11 Gordillo Altamirano FL, Barr JJ. Phage therapy in the postantibiotic era. *Clin Microbiol Rev*. 2019;32. https://doi.org/10.1128/CMR.00066-18.
12 Hua Y, Luo T, Yang Y, et al. Phage therapy as a promising new treatment for lung infection caused by carbapenem-resistant *Acinetobacter baumannii* in mice. *Front Microbiol*. 2017;8:2659.
13 Jeon J, Park JH, Yong D. Efficacy of bacteriophage treatment against carbapenem-resistant *Acinetobacter baumannii* in *Galleria mellonella* larvae and a mouse model of acute pneumonia. *BMC Microbiol*. 2019;19:70.
14 Leshkasheli L, Kutateladze M, Balarjishvili N, et al. Efficacy of newly isolated and highly potent bacteriophages in a mouse model of extensively drug-resistant *Acinetobacter baumannii* bacteraemia. *J Glob Antimicrob Resist*. 2019;19:255–261.
15 Wintachai P, Naknaen A, Pomwised R, Voravuthikunchai SP, Smith DR. Isolation and characterization of Siphoviridae phage infecting extensively drug-resistant *Acinetobacter baumannii* and evaluation of therapeutic efficacy in vitro and *in vivo*. *J Med Microbiol*. 2019;68:1096–1108.
16. Regeimbal JM, Jacobs AC, Corey BW, et al. Personalized therapeutic cocktail of wild environmental phages rescues mice from *Acinetobacter baumannii* wound infections. *Antimicrob Agents Chemother*. 2016;60:5806–5816.
17 Schooley RT, Biswas B, Gill JJ, et al. Development and use of personalized bacteriophage-based therapeutic cocktails to treat a patient with a disseminated resistant *Acinetobacter baumannii* infection. *Antimicrob Agents Chemother*. 2017;61:e00954-17.
18 Tan X, Chen H, Zhang M, et al. Clinical experience of personalized phage therapy against carbapenem-resistant *Acinetobacter baumannii* lung infection in a patient with chronic obstructive pulmonary disease. *Front Cell Infect Microbiol*. 2021;11: 631585.
19 Wu N, Dai J, Guo M, et al. Pre-optimized phage therapy on secondary *Acinetobacter baumannii* infection in four critical COVID-19 patients. *Emerg Microbes Infect*. 2021;10:612–618.
20 Nir-Paz R, Gelman D, Khouri A, et al. Successful treatment of antibiotic-resistant, poly-microbial bone infection with bacteriophages and antibiotics combination. *Clin Infect Dis*. 2019;69:2015–2018.
21 LaVergne S, Hamilton T, Biswas B, Kumaraswamy M, Schooley RT, Wooten D. Phage therapy for a multidrug-resistant *Acinetobacter baumannii* craniectomy site infection. *Open Forum Infect Dis*. 2018;5:ofy064.
22 Doern CD. When does 2 plus 2 equal 5? A review of antimicrobial synergy testing. *J Clin Microbiol*. 2014;52:4124.
23 Huff WE, Huff GR, Rath NC, Balog JM, Donoghue AM. Therapeutic efficacy of bacteriophage and Baytril (enrofloxacin) individually and in combination to treat colibacillosis in broilers. *Poult Sci*. 2004;83:1944–1947.
24 Comeau AM, Tetart F, Trojet SN, Prere MF, Krisch HM. Phage-antibiotic synergy (PAS): beta-lactam and quinolone antibiotics stimulate virulent phage growth. *PLoS One*. 2007;2:e799.
25 Al-Anany AM, Fatima R, Hynes AP. Temperate phage-antibiotic synergy eradicates bacteria through depletion of lysogens. *Cell Rep*. 2021;35: 109172.
26 Torres-Barceló C, Hochberg ME. Evolutionary rationale for phages as complements of antibiotics. *Trends Microbiol*. 2016;24:249–256.
27 Burmeister AR, Turner PE. Trading-off and trading-up in the world of bacteria-phage evolution. *Curr Biol*. 2020;30:R1120–R11R4.
28 Mangalea MR, Duerkop BA. Fitness trade-offs resulting from bacteriophage resistance potentiate synergistic antibacterial strategies. *Infect Immun*. 2020;88:e00926-19.
29 Tagliaferri TL, Jansen M, Horz H-P. Fighting pathogenic bacteria on two fronts: phages and antibiotics as combined strategy. *Front Cell Infect Microbiol*. 2019;9:22.
30 Jansen M, Wahida A, Latz S, et al. Enhanced antibacterial effect of the novel T4-like bacteriophage KARL-1 in combination with antibiotics against multi-drug resistant *Acinetobacter baumannii*. *Sci Rep*. 2018;8:14140.
31 Styles KM, Thummeepak R, Leungtongkam U, et al. Investigating bacteriophages targeting the opportunistic pathogen *Acinetobacter baumannii*. *Antibiotics*. 2020;9:200. (Basel).
32 Blasco L, Ambroa A, Lopez M, et al. Combined use of the Ab105-2$\varphi\Delta$CI lytic mutant phage and different antibiotics in clinical isolates of multi-resistant *Acinetobacter baumannii*. *Microorganisms*. 2019;7:556.
33 Gordillo Altamirano F, Forsyth JH, Patwa R, et al. Bacteriophage-resistant *Acinetobacter baumannii* are resensitized to antimicrobials. *Nat Microbiol*. 2021;6:157–161.
34 Adams MD, Goglin K, Molyneaux N, et al. Comparative genome sequence analysis of multidrug-resistant *Acinetobacter baumannii*. *J Bacteriol*. 2008;190:8053–8064.
35 Kenyon JJ, Hall RM. Variation in the complex carbohydrate biosynthesis loci of *Acinetobacter baumannii* genomes. *PLoS One*. 2013;8: e62160.
36 Gordillo Altamirano FL, Barr JJ. Screening for lysogen activity in therapeutically relevant bacteriophages. *Bio-protoc*. 2021;11:e3997.
37 Bonilla N, Rojas MI, Netto Flores Cruz G, Hung S-H, Rohwer F, Barr JJ. Phage on tap–a quick and efficient protocol for the preparation of bacteriophage laboratory stocks. *PeerJ*. 2016;4:e2261.
38 Harris G, Holbein BE, Zhou H, Xu HH, Chen W. Potential mechanisms of mucin-enhanced *Acinetobacter baumannii* virulence in the mouse model of intraperitoneal infection. *Infect Immun*. 2019;87: e00591-19.
39 Acred P. Therapeutic and kinetic properties of ceftazidime in animals. *Infection*. 1983;11:S44–S48.
40 Richards DM, Ceftazidime BRN. A review of its antibacterial activity, pharmacokinetic properties and therapeutic use. *Drugs*. 1985;29:105–161.
41 Andrews S. FastQC: A Quality Control Tool For High Throughput Sequence data. [Internet] Cambridge, UK: Babraham Bioinformatics; [2010; cited November 2020]. Available from: http://www.bioinformatics.babraham.ac.uk/projects/fastqc/.
42 Bolger AM, Lohse M, Usadel B. Trimmomatic: a flexible trimmer for Illumina sequence data. *Bioinformatics*. 2014;30:2114–2120.
43 Thorvaldsdóttir H, Robinson JT, Mesirov JP. Integrative Genomics viewer (IGV): high-performance genomics data visualization and exploration. *Brief Bioinform*. 2013;14:178–192.
44 Wiegand I, Hilpert K, Hancock RE. Agar and broth dilution methods to determine the minimal inhibitory concentration (MIC) of antimicrobial substances. *Nat Protoc*. 2008;3:163–175.
45 Gu Liu C, Green SI, Min L, et al. Phage-antibiotic synergy is driven by a unique combination of antibacterial mechanism of action and stoichiometry. *mBio*. 2020;11:e01462-20.
46 Percie du Sert N, Hurst V, Ahluwalia A, et al. The ARRIVE guidelines 2.0: Updated guidelines for reporting animal research. *PLoS Biol*. 2020;18: e3000410.
47 Ballouz T, Aridi J, Afif C, et al. Risk factors, clinical presentation, and outcome of *Acinetobacter baumannii* bacteremia. *Front Cell Infect Microbiol*. 2017;7:156.
48 Papathanakos G, Andrianopoulos I, Papathanasiou A, Priavali E, Koulenti D, Koulouras V. Colistin-resistant *Acinetobacter baumannii* bacteremia: a serious threat for critically ill patients. *Microorganisms*. 2020;8:287.
49 Singh JK, Adams FG, Brown MH. Diversity and function of capsular polysaccharide in *Acinetobacter baumannii*. *Front Microbiol*. 2019;9:3301.
50 Kenyon JJ, Shashkov AS, Senchenkova SN, et al. *Acinetobacter baumannii* K11 and K83 capsular polysaccharides have the same 6-deoxy-l-talose-containing pentasaccharide K units but different linkages between the K units. *Int J Biol Macromol*. 2017;103:648–655.
51 Fantin B, Carbon C. *In vivo* antibiotic synergism: contribution of animal models. *Antimicrob Agents Chemother*. 1992;36:907–912.
52 Torella JP, Chait R, Kishony R. Optimal drug synergy in antimicrobial treatments. *PLoS Comput Biol*. 2010;6: e1000796.
53 Knezevic P, Curcin S, Aleksic V, Petrusic M, Vlaski L. Phage-antibiotic synergism: a possible approach to combatting *Pseudomonas aeruginosa*. *Res Microbiol*. 2013;164:55–60.
54 Gordillo Altamirano FL, Barr JJ. Unlocking the next generation of phage therapy: the key is in the receptors. *Curr Op Biotechnol*. 2021;68:115–123.
55 Pirnay J-P, Ferry T, Resch G. Recent progress toward the implementation of phage therapy in western medicine. *FEMS Microbiol Rev*. 2022;46:fuab040.

56 Ratelade J, Verkman AS. Inhibitor(s) of the classical complement pathway in mouse serum limit the utility of mice as experimental models of neuromyelitis optica. *Mol Immunol*. 2014;62:104–113.

57 Chan BK, Sistrom M, Wertz JE, Kortright KE, Narayan D, Turner PE. Phage selection restores antibiotic sensitivity in MDR *Pseudomonas aeruginosa*. *Sci Rep*. 2016;6:26717.

58 Chatterjee A, Johnson CN, Luong P, et al. Bacteriophage resistance alters antibiotic-mediated intestinal expansion of enterococci. *Infect Immun*. 2019;87:e00085-19.

59 Oechslin F. Resistance development to bacteriophages occurring during bacteriophage therapy. *Viruses*. 2018;10:351.

60 Burmeister AR, Fortier A, Roush C, et al. Pleiotropy complicates a trade-off between phage resistance and antibiotic resistance. *Proc Natl Acad Sci U S A*. 2020;117:11207.

61 Wright RCT, Friman V-P, Smith MCM, Brockhurst MA. Resistance evolution against phage combinations depends on the timing and order of exposure. *mBio*. 2019;10. https://doi.org/10.1128/mBio.01652-19.

62 Bai J, Dai Y, Farinha A, et al. Essential gene analysis in *Acinetobacter baumannii* by high-density transposon mutagenesis and CRISPR interference. *J Bacteriol*. 2021;203:e00565-20.

63 Bichet MC, Chin WH, Richards W, et al. Bacteriophage uptake by mammalian cell layers represents a potential sink that may impact phage therapy. *iScience*. 2021;24: 102287.

64 Dąbrowska K. Phage therapy: What factors shape phage pharmacokinetics and bioavailability? Systematic and critical review. *Med Res Rev*. 2019;39:2000–2025.

65 Song L, Yang X, Huang J, et al. Phage selective pressure reduces virulence of hypervirulent *Klebsiella pneumoniae* through mutation of the *wzc* gene. *Front Microbiol*. 2021;12: 739319.

66 Engeman E, Freyberger HR, Corey BW, et al. Synergistic killing and re-sensitization of *Pseudomonas aeruginosa* to antibiotics by phage-antibiotic combination treatment. *Pharmaceuticals*. 2021;14:184. (Basel).

67 Wang X, Loh B, Gordillo Altamirano F, Yu Y, Hua X, Leptihn S. Colistin-phage combinations decrease antibiotic resistance in *Acinetobacter baumannii* via changes in envelope architecture. *Emerg Microbes Infect*. 2021;10:2205–2219.